Trapping probability analysis of a DNA trap using electric and hydrodrag force fields in tapered microchannels

Yuichi Tomizawa,[1] Eiichi Tamiya,[2] and Yuzuru Takamura[1]
[1]*School of Materials Science, Japan Advanced Institute of Science and Technology, 1-1 Asahidai, Nomi, Ishikawa 923-1292, Japan*
[2]*School of Engineering, Osaka University, 1-2 Yamadaoka, Suita, Osaka 565-0871, Japan*
(Received 6 August 2008; revised manuscript received 3 March 2009; published 8 May 2009)

This paper describes a quantitative analysis of the trapping probability for the DNA trap, which is a method of trapping and concentrating DNA in a tapered microchannel by electric and hydrodrag force fields. In order to calculate the trapping probability, a series of connections of triangle-shaped taper stages was used. The fluorescent intensity of trapped DNA molecules at each stage was measured. The trapping probability per stage was calculated from the distribution of the fluorescent increase rate along with the stage number. The trapping probabilities were measured as a function of DNA size, electric field, and average hydraulic velocity. The electric field that gives a trap probability of 0.5 was found to be proportional to the average hydraulic velocity for all DNA sizes. For all measured conditions and accuracy, the trapping probability was found to be determined only by the ratio of the electric field to the average hydraulic velocity. These results reveal that the DNA trap is not simply caused by balance between the dielectrophoresis and hydrodrag forces.

DOI: 10.1103/PhysRevE.79.051902 PACS number(s): 87.80.−y, 87.15.−v, 87.90.+y

I. INTRODUCTION

In recent years, technologies that miniaturize chemical or biochemical analysis methods onto chips with areas of several square centimeters are being developed and opening up new application areas, such as single-cell analysis, ultracompact analyzers, next-generation DNA sequencers, and cell/DNA array chips. These technologies also create new research fields to study the functions enabled by utilizing their fine structures or limited spaces in miniaturized system. For example, there are some reports on manipulating DNA using artificial nanostructures, such as nanopillars [1,2], entropic traps [3], curved nanochannels [4], nanopores [5], etc. There is also great interest in revealing the mechanisms underlying such new functions.

We have been studying a phenomena "DNA trap," which was found in 2002 [6]. A buffer solution containing DNA is introduced into a chip with a triangle-shaped tapered microchannel. When electric and hydrodrag forces are applied to the DNA simultaneously in opposite directions, the DNA is trapped near the narrowest position of the tapered microchannel (Fig. 1). Several characteristics of the DNA trap have been discovered in a series of study [6–11]. The DNA molecules are trapped with a dynamic motion in a circular orbit. Charged polymerlike molecules can also be trapped. To trap a molecule, the two forces acting on the molecule should be nearly balanced. Therefore, the trap is molecule selective and tunable; thus it can be used to extract a specific molecule from a mixture. If the two forces are not completely balanced, molecules can still move, except through the narrowest position. Here, the DNA comes from upstream to the narrowest position and stays there. That means this trap can be used to concentrate on specific molecules. Small molecules can be trapped by relatively large structures; i.e., a 1 kbp DNA molecule can be trapped by a 10 μm channel. This feature is advantageous as it avoids clogging up the microchannel. Trapped molecules can be released immediately when one of the forces is removed. We expect that the trap can be used for the pretreatment of polymerlike molecules on a microfluidic chip, such as the extraction and purification of DNA/RNA from cell lysate at the single-cell level.

For further studies, such as optimizing the trap abilities or discussing the mechanism, a quantitative analysis of the trap is necessary. As the simplest quantitative parameter, in this paper we introduce a trapping probability of the DNA trap, which is the probability that a DNA molecule entering the trap position is trapped there. However, it is arduous to measure the trapping probability by counting each molecule and whether they are trapped or not trapped to a sufficient number for reliable accuracy at various trap conditions.

Within this paper, a statistic analysis method of the trapping probability is developed. Avoiding an arduous procedure, this method can account for the behavior of a large number of DNA molecules at once. The series connection of the triangle-shaped taper stages is used for the trap channel. The increase rate of trapping DNA at each stage is measured. The trapping probabilities per stage are calculated from the increase rate distribution along with the stage number. The trapping probabilities are measured as a function of DNA size, electric field, and average hydraulic velocity. The measured trapping probabilities are discussed together with the

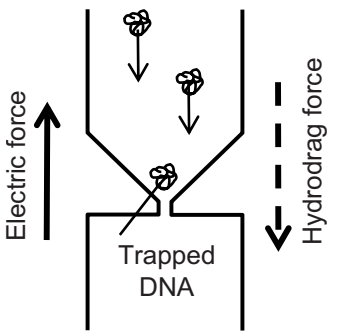

FIG. 1. Schematic of DNA trapping.

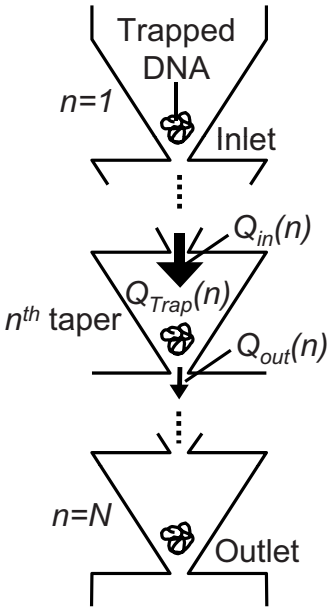

FIG. 2. Schematic of the analysis model. $Q_{in}(n)$ indicates the quantity of DNA flow into the nth taper. $Q_{Trap}(n)$ expresses the quantity of trapped DNA in the nth taper. $Q_{out}(n)$ represents the quantity of DNA flow out from the nth taper.

values for the electric field and average hydrovelocity in terms of the mechanism of the trap.

II. ANALYSIS METHOD FOR THE TRAPPING PROBABILITY OF THE DNA TRAP

Let us consider a situation where a constant differential pressure (ΔP) and certain value of dc voltage (V_a) are applied to a tapered microchannel with a series of triangle-shaped tapered stages (Fig. 2). In Fig. 2, the inlet and outlet are defined by the direction of the pressure-driven flow due to the difference in pressure between the ends of the microchannel. $Q_{in}(n)$ is the total quantity of DNA molecules flowing in the nth stage taper, and $q_{in}(n)$ is the amount of DNA molecules flowing in the nth stage taper per unit time. In addition, $Q_{out}(n)$ is the total quantity of DNA molecules flowing out from the nth stage taper, and $q_{out}(n)$ is the amount of DNA molecules flowing out from the nth stage taper per unit time.

From these definitions, we get the two equations shown below,

$$\frac{d}{dt}Q_{in}(n) = q_{in}(n), \tag{1}$$

$$\frac{d}{dt}Q_{out}(n) = q_{out}(n), \tag{2}$$

where $1 \le n \le N$, $N=10$ in the actual experiments (Sec. III).

If the quantity of trapped DNA molecules in the nth stage taper is represented by $Q_{Trap}(n)$, the quantity of trapped DNA molecules in the nth stage taper per unit time is expressed by the next formula,

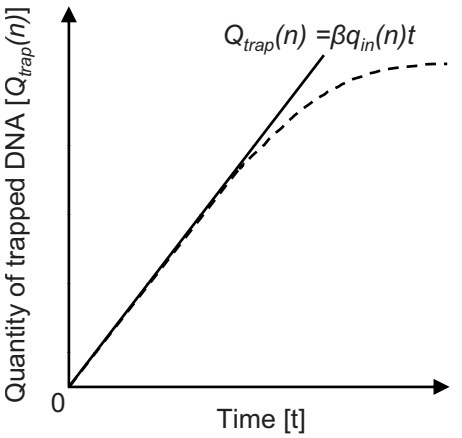

FIG. 3. Assumed time evolution of a trapped DNA quantity at the single taper stage. The dashed curve indicates a quantity of trapped DNA molecules. The solid line is a tangent to the curve when time t is close to 0.

$$\frac{d}{dt}Q_{Trap}(n) = q_{in}(n) - q_{out}(n). \tag{3}$$

Here,

$$q_{in}(n+1) = q_{out}(n) \quad (1 \le n \le N-1). \tag{4}$$

The DNA flow rate, or the flow of DNA molecules per unit time, in the straight region ($n=0$) of the microchannel at the inlet side is defined as q_0; this value is determined only by ΔP and V_a. Therefore, the flow of DNA molecules into the first taper ($n=1$) per unit time is constant,

$$q_{in}(1) = q_0 \cdots const. \tag{5}$$

Here, the trapping probability β and escape rate γ are defined as follows. Each DNA molecule flowing into a taper stage is trapped there at a probability β or flows out from the taper stage immediately at a probability $(1-\beta)$. Once trapped, each DNA molecule escapes from the taper stage at the rate γ. The β and γ are a function of ΔP and V_a. Based on the above two definitions, $q_{out}(n)$ can be expressed as the next equation,

$$q_{out}(n) = (1-\beta)q_{in}(n) + \gamma Q_{Trap}(n) \tag{6}$$

We obtain the next equation by substituting Eq. (6) for Eq. (3),

$$\frac{d}{dt}Q_{Trap}(n) = \beta q_{in}(n) - \gamma Q_{Trap}(n). \tag{7}$$

We define $t=0$ at the start point of trapping DNA so that $Q_{Trap}(n)=0$ when time $t=0$. The predicted evolution of $Q_{Trap}(n)$ is shown as a dashed curve in Fig. 3. At $t=0$, Eq. (7) is simplified as

$$\frac{d}{dt}Q_{Trap}(n) = \beta q_{in}(n) \quad (t=0). \tag{8}$$

This corresponds to the tangent (solid line) of the curve at $t=0$ in Fig. 3.

From Eqs. (4) and (6), we get $q_{in}(n)=q_{out}(n-1)=(1-\beta)q_{in}(n-1)$ at $(t\geq 0, 2\leq n\leq N)$, and by applying this relation to the above equation, we obtain

$$\frac{d}{dt}Q_{Trap}(n) = \beta q_{in}(n) = \beta(1-\beta)q_{in}(n-1)$$

$$= \cdots = \beta(1-\beta)^{n-1}q_0 \quad (t=0). \tag{9}$$

Taking the natural logarithm of each side of Eq. (9), we obtain the next formula,

$$\log\left\{\frac{d}{dt}Q_{Trap}(n)\right\} = (n-1)\log(1-\beta) + \log \beta q_0 \quad (t=0). \tag{10}$$

Here, let us consider the relation between the measured fluorescence intensity and quantity of DNA. The YOYO-1, a fluorescence dye used in this paper, is known to be intercalated to the DNA base pair at a constant density. When the length of DNA is constant, the observed fluorescence intensity from a DNA molecule is constant. Thus, the measured fluorescence intensity is proportional to the DNA quantity (or number of DNA molecules). Based on this relation, the measured fluorescence intensity of trapped DNA molecules at the nth taper $I_{obs}(n)$ is expressed by

$$I_{obs}(n) = \alpha Q_{Trap}(n) + I_b(n), \tag{11}$$

where α is a proportional constant. Experimentally, a photobleaching effect must be considered. We discussed photobleaching in Sec. IV. I_b is the background,

$$\frac{d}{dt}I_{obs}(n) = \alpha\frac{d}{dt}Q_{Trap}(n). \tag{12}$$

Substitute the above equation into Eq. (10),

$$\log\left\{\frac{d}{dt}I_{obs}(n)\right\}$$

$$= n\log(1-\beta) + \log \beta q_0 + \log \alpha - \log(1-\beta),$$

$$\log\left\{\frac{d}{dt}I_{obs}(n)\right\} = n\log(1-\beta) + C \quad (t=0), \tag{13}$$

where $C=\log \beta q_0+\log \alpha-\log(1-\beta)$.

From slope k of a line obtained by plotting $\log\{\frac{d}{dt}I_{obs}(n)\}$ with respect to n,

$$\log(1-\beta) = k,$$

$$\beta = 1 - e^k \quad (t=0). \tag{14}$$

We can estimate the trapping probability β.

III. DNA TRAP EXPERIMENT

The required microchannel for the trap experiment was patterned using an electron beam (EB) lithography system (ELS-3300, Elionix) on an EB resist coated chromium-glass substrate (DUFQ-3006p, Ulcoat Tokyo). A quartz glass plate was soaked in a 4:1 mixer solution (piranha cleaning solution) of sulfuric acid and hydrogen peroxide and heated for 1 day at 150 °C to clean the surface. A 1-μm-thick layer of laminar chromium was sputtered (MNS-2000, ULVAC) onto the glass surface, and positive photoresist (OFPR-800 LB, Tokyo Ohka Kogyo) was coated onto the chromium surface with a spin coater (1H-DX2, Mikasa). UV light exposure was performed through the above-mentioned photomask on the photoresist-coated surface with photolithography equipment (MJB3, Karl Suss). After developing the OFPR-800, unnecessary chromium was removed with wet etchant (MPM-E30, IncTec). The remaining chromium layer was used as a mask for the dry etching process (RIE-200iPB, SAMCO), and a 1-μm-depth channel was carved. For an injection of the sample solution, a 2 mm diameter hole was made using an ultrasonic machine (Sonopet 100B, Seidensya electronics) as a reservoir. All the chromium was removed from the glass surface by the etchant; the glass substrate (with channel and reservoir) and a cover glass were then soaked in piranha cleaning solution to remove impurities. The glass substrate and cover glass were bonded to each other after we dropped 1% hydrofluoric acid solution on each surface. Fabrication of the glass chip was completed by applying adequate pressure using a specialized jig in a 65 °C oven for 12 h. The entire chip fabrication process described here was carried out in a clean room facility.

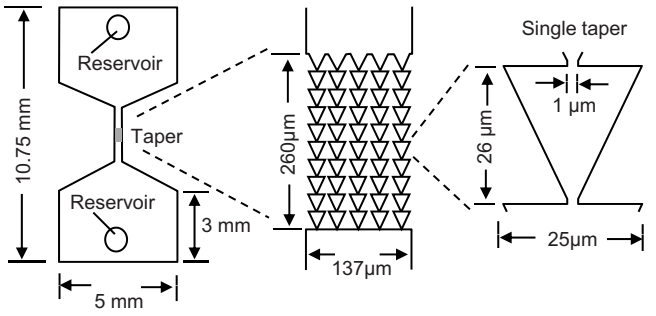

FIG. 4. Structure of the tapered microchannel. The depth is 1 μm and the distance between the two reservoir holes is about 1 cm (left figure). Each line for the series of tapered structures consists of ten connected triangular tapers (middle figure). The narrowest part of the single tapered microchannel is 1 μm (right figure).

Figure 4 shows the structure of the fabricated glass chip. The depth is 1 μm throughout this microchannel. The distance between the centers of the 2 mm diameter reservoir holes is about 1 cm (left figure). There are five lines of continuous taper structures in the middle of the microchannel; each line is separated by 3 μm spaces at the closest points. A single line for a continuous taper structure consists of ten triangular-shaped tapers (middle figure). Figure 4 (right) shows a single triangle-shaped taper structure: 26 μm height, 1 μm width at its narrowest, and 25 μm width at its widest.

Three different commercially available molecular weight DNA molecules (166 kbp T4, 48 kbp lambda, and 7.3 kbp M13mp from Nippon gene) were independently used in trap experiments. For fluorescent labeling of the DNA samples, YOYO-1 molecules (Ex. 491 nm, Em. 509 nm, molecular

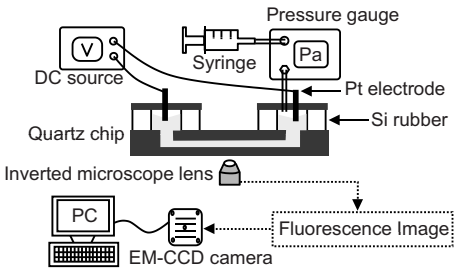

FIG. 5. Schematic of experimental setup. Fluorescent-labeled DNA was trapped in a tapered microchannel by applying direct-current voltage and differential pressure simultaneously to both ends of the microchannel.

probe) was mixed with DNA samples at a mixing rate of DNA bp: YOYO-1 molecule 5:1, and stored in a refrigerator at 3 °C for 24 h. Intercalated T4, lambda, and M13mp9 were prepared at molar concentrations of 0.604, 2.06, and 13.16 pmol/L, respectively, in a 0.5 tris-borate Ethylenediaminetetraacetic acid (TBE, pH 8.2) buffer. This buffer contained 300 μmol/L polyvinylpyrrolidone (PVP) as a blocking reagent of electro-osmosis; it also contained 0.013 mol/L glucose, 0.83 μmo/L catalase, and 1.33 μmol/L glucose oxidase to protect the DNA from fragmentation by dissolved oxygen. Thus, 0.02 μmol/L of YOYO-1 molecules existed in each DNA length solution; based on the above-mentioned ratio of 5:1 (DNA bp and YOYO-1 molecules), 6.02×10^{12} bp DNA was contained in the 100 μL buffer solution.

The prepared buffer solution was introduced into a reservoir at the inlet; reservoirs were sealed by small glass slides with a pressure tube and platinum electrode. The required value for the difference in pressure between the ends of the channel was adjusted to an accuracy of 1 hPa, and the dc voltage was adjusted to an accuracy of 1 V. Trapped DNA molecules in the tapered microchannel were observed via fluorescent microscope (IX 70, Olympus) while differential pressure (ΔP) and dc voltage (V_a) were simultaneously applied in opposite directions (Fig. 5). Differential pressures of 20–100 hPa and voltages of 0–30 V were used in the trap experiments. The data for fluorescence images (Fig. 6) from

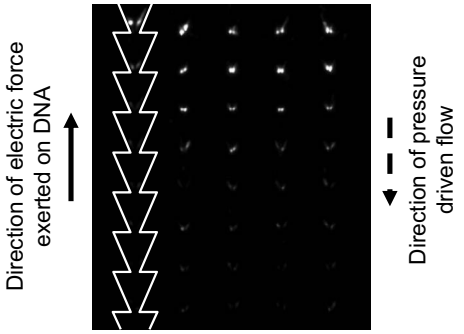

FIG. 6. Typical snapshots for fluorescence images of trapped DNA in the series of taper shape channels for lambda DNA (48 kbp) at $t=10.4$ s, $\Delta P=70$ hPa, and $V=11$ V. The white lines indicate the position of one series of the tapers. The white bright spots are trapped DNA molecules.

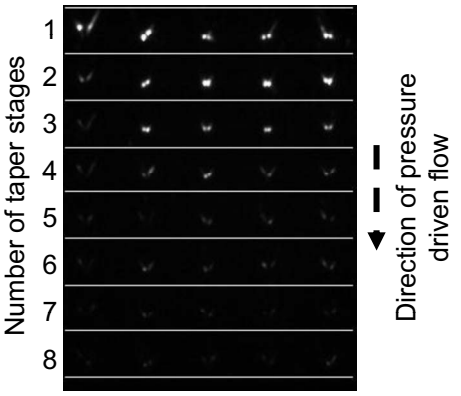

FIG. 7. Integration areas to measure the fluorescence intensity of each taper stage. The white lines separate the fluorescent spots of trapped DNA in Fig. 6 into each taper stage. The numbers of the taper stages are indicated at the left side of the figure.

an electron multiplier-CCD camera (C9100, Hamamatsu Photonics) were stored in a PC, and the fluorescence intensity per frame was analyzed (Fig. 6) using SIMPLE-PCI software (Leeds Instruments). Here, a single frame is nearly equal to 0.139 s in time. The DNA trapping probability, discussed in Sec. II for different length DNA molecules (T4: 166 kbp; lambda: 48.5 kbp; M13mp9: 7.2 kbp), was calculated from the analyzed fluorescent intensities.

IV. RESULTS AND DISCUSSION

Figure 6 is a typical snapshot for the fluorescence images of trapped DNA in the series of tapered triangle-shaped channels. Here, the molecules are lambda DNA (48 kbp) with $t=10.4$ s, $\Delta P=70$ hPa, and $V_a=11$ V. The observation area corresponds to the middle figure in Fig. 4. White lines indicate the position for one series of the tapers. The solid arrow indicates the direction of electric force exerted on the DNA molecules, and the dashed arrow indicates the direction of the pressure-driven flow. The white bright spots are trapped DNA molecules. They come from the upper side at a constant rate and are being trapped and accumulating at those spots, i.e., near the narrowest position of each tapered triangle-shaped channel. The $I_{obs}(n)$ for each spot was found to gradually weaken from the upper to lower sides. The trap probability for each taper is considered to be nearly equal, at least initially, so the gradation means that the total amount of DNA entering each stage was changing.

Figure 7 indicates the integration areas to measure $I_{obs}(n)$. White lines separate the fluorescent spots of trapped DNA in Fig. 7 into each taper stage. As shown on the left side of this figure, the number of taper stages is counted from the inlet to the outlet along the stream of pressure-driven flow.

Figure 8 shows the typical time dependence for a measured $I_{obs}(n)$. This figure is the result for lambda DNA at 62 hPa and 11 V. The eight curves indicate the fluorescence intensities of trapped DNA molecules at the first to eighth taper stages in order from the top, respectively. The zero frame corresponds to $t=0$ when voltage was applied, i.e., before this, only the pressure-driven flow was present. From

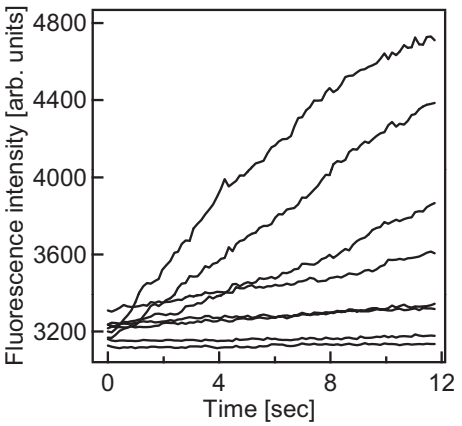

FIG. 8. Typical time dependence of measured fluorescence intensity for lambda DNA at 62 hPa and 11 V. The eight curves from the top are for the first to eighth taper stages, respectively. The zero frame corresponds to $t=0$ when voltage was applied.

these curves, the fluorescence increase rate $(d/dt)I_{obs}(n)$ at $t=0$ corresponding to the left side of Eq. (12) can be determined. During the time period of 0–8.34 s (0–60 frames), the fluorescent intensities increase approximately linearly with time. Therefore, we can estimate $(d/dt)I_{obs}(n)$ at $t=0$ as the slope of the linear fitting of those curves at this period. In almost every case where a trap occurred, the linear period of the curves was observed in the earlier time range (0 to several seconds). The extent of the linear periods varied with the trap condition. Therefore, the periods used for analysis have to be chosen carefully for every condition. We analyzed the trap probabilities only for cases where the linear period was clearly observed; the cases without it were removed from further study. The linearity also suggests that the photobleaching of YOYO-1 is negligible for this short period. In order to estimate the effect of photobleaching on $I_{obs}(n)$, we also measured the fluorescence decay rate by photobleaching in actual our setup when flow was stopped. The estimated effect was in the order of a few percents and negligible compared to our experimental error.

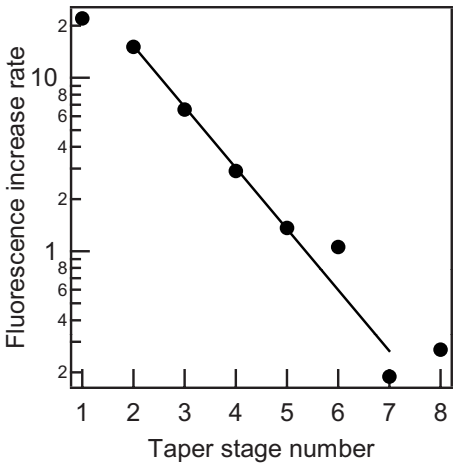

FIG. 9. Increase in the rate of fluorescence intensity versus the taper-stage number. The solid line indicates linear fitting for data of the second to seventh taper stages.

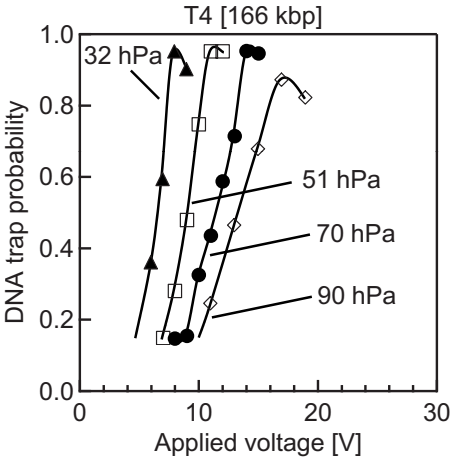

FIG. 10. Calculated trapping probabilities for T4 DNA at various differential pressures plotted as a function of applied direct-current voltage.

Figure 9 plots the increase in rate versus the taper-stage number. Here, the vertical and horizontal axes correspond with the left side of Eq. (13) in Sec. II and n, respectively. The solid line indicates fitting of the plots for the second to seventh taper stages. The slope of this fitting line corresponds to k of Eq. (14). In this figure, the plots for the first stage and sixth to eighth stages deviated from the fitting line. The former is reasonable because the first stage is directly connected to the straight microchannel, and the force fields in the first stage should be slightly different from the others. We considered the latter to be due to noise because the fluorescence intensities for these stages were very low. The plots for the second to fifth stages correlate well to the line. This fact suggests that our analysis method is appropriate for these cases.

Finally, the tapping probabilities were calculated from k using Eq. (14). Figures 10–12 represent the DNA trapping probabilities for T4, lambda, and M13mp9 DNA, respectively. The four curves of each figure indicate the change in trapping probability with the voltage at various ΔP. The re-

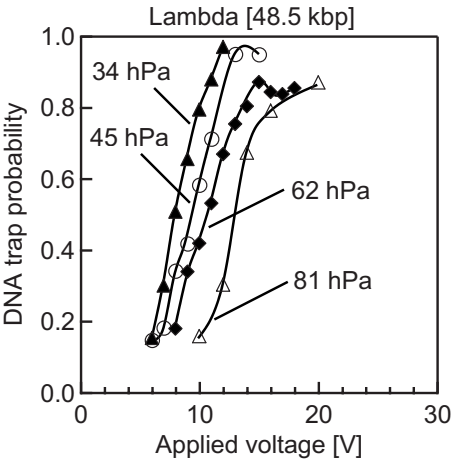

FIG. 11. Calculated trapping probabilities for lambda DNA at various differential pressures plotted as a function of applied direct-current voltage.

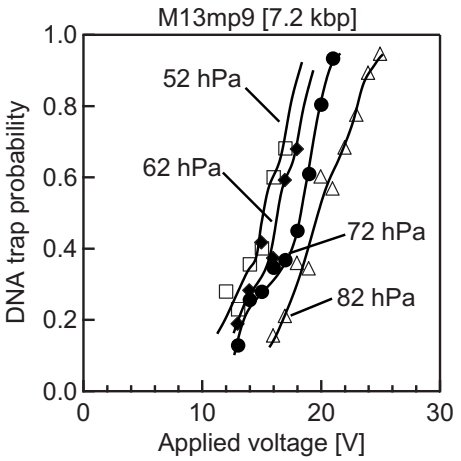

FIG. 12. Calculated trapping probabilities for M13mp9 DNA at various differential pressures plotted as a function of applied direct-current voltage.

sponse to voltage change by the trapping probabilities increased with sensitivity. In comparing Figs. 10–12, it is interesting to note that the required ΔP and V_a for trapping short DNA were higher than those required for long DNA molecules.

For further discussion, ΔP and V_a were converted into relevant physical units of the representative flow velocity and electric field. For the representative flow velocity, we chose the average hydraulic flow velocity ($\langle u_h \rangle$) of the pressure-driven flow at the taper region. For a given fluid, the flow velocity should be determined only by ΔP in the microchannel of the same geometry so that it should be calculated from ΔP. The flow velocity, however, varies very sensitively to the diameter of the microchannel (inversely with the fourth powered of it). The fabrication accuracy of the microchannel used for each measurement is important. Here, for better quantitative analysis, we used $\langle u_h \rangle$ measured for each condition instead of $\langle u_h \rangle$ calculated from ΔP. Experimentally, $\langle u_h \rangle$ was measured at each condition of ΔP and DNA size by averaging the velocity of DNA molecules released by removing V_a after they were trapped once by V_a and ΔP. The measured $\langle u_h \rangle$ is listed in Table I. For the representative electric field, we chose the strength of the electric field (E_s) for the straight part of the channel in Fig. 4. E_s is less sensitive to the fabrication accuracy of the microchannel than $\langle u_h \rangle$. Here, E_s is calculated by two-dimensional (2D) numerical simulation using the simulation software COMSOL (COMSOL, Inc.). We obtained a relationship of $E_s = 231 V_a$.

TABLE I. Results of measured $\langle u_h \rangle$ at each ΔP.

T4		Lambda		M13mp9	
ΔP (hPa)	$\langle u_h \rangle$	ΔP (hPa)	$\langle u_h \rangle$	ΔP (hPa)	$\langle u_h \rangle$
32	30	34	28	52	68
51	39	45	34	62	73
70	53	62	46	72	85
90	69	81	61	82	107

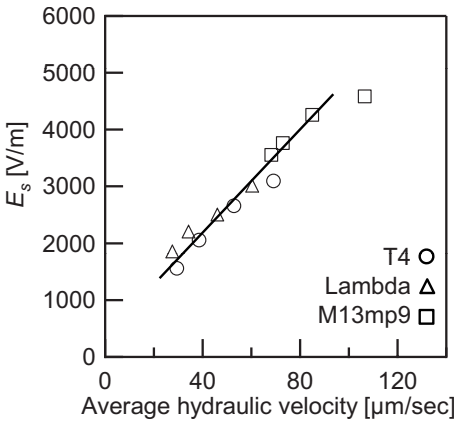

FIG. 13. $E_{s,0.5}$ and hydraulic velocity at a trapping probability of 0.5. This figure indicates a plot of the $E_{s,0.5}$ as a function of $\langle u_h \rangle$ for each DNA size. The hydraulic velocity $\langle u_h \rangle$ is measured at each condition of ΔP and DNA size by averaging the velocity of DNA molecules released by removing V_a after they are trapped once by V_a and ΔP. For the representative electric field, we chose the strength of the electric field (E_s) at the straight part of the channel in Fig. 4. For each $\langle u_h \rangle$ and DNA size, we obtained the $E_{s,0.5}$ where the trapping probability was 0.5.

For each $\langle u_h \rangle$ and DNA size, we obtained an E_s where the trapping probability=0.5($E_{s,0.5}$). Figure 13 is a plot of $E_{s,0.5}$ as a function of $\langle u_h \rangle$ for each DNA size. Interestingly, $E_{s,0.5}$ is approximately proportional to $\langle u_h \rangle$ and all plots for the different DNA sizes are on a line. Some groups have reported on trapping DNA using dielectricphoresis (DEP) [12–15]. Most DEP experiments use alternative current (ac); however, DEP also occurs with direct current (dc). In general, however, the strength of the DEP force is proportional to the gradient of the square of the electric field. If our trap is simply caused by balance between the dc-DEP and hydrodrag forces, then $E_{s,0.5}$ should be proportional to the square root of $\langle u_h \rangle$. However, our results do not show this. This reveals that our trap is not simply caused by the balance between the dc-DEP force and hydrodrag force. Another mechanism is required to explain the DNA trapping for our case.

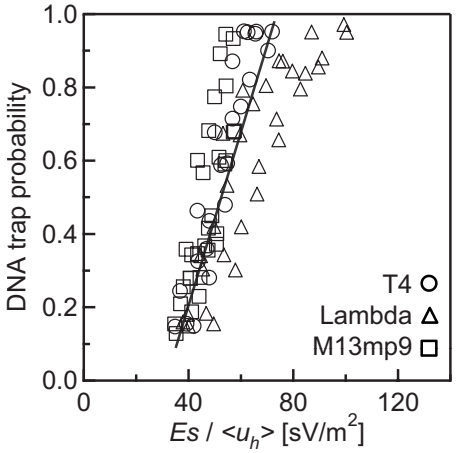

FIG. 14. DNA trap probability as a function of $E_s/\langle u_h \rangle$.

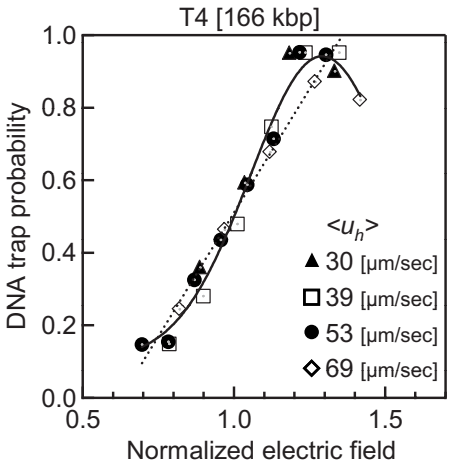

FIG. 15. Trapping probability of T4 DNA versus normalized voltage. The voltage was normalized at the value of 0.5 for the trapping probability at each pressure difference shown in Fig. 10. The solid curve and dotted line are the (A) Gauss and (B) linear functions for all plot marks, respectively.

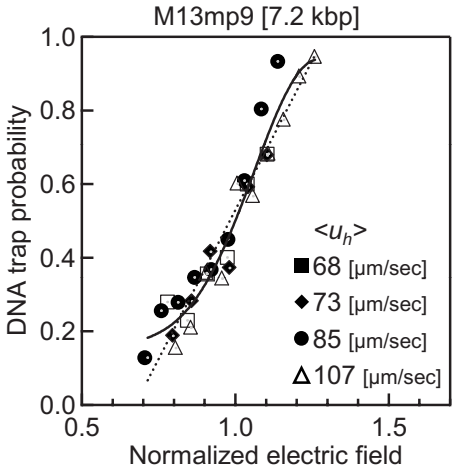

FIG. 17. Trapping probability of M13mp9 DNA versus normalized voltage. The voltage was normalized at the value of 0.5 for the trapping probability at each pressure difference shown in Fig. 12. The solid curve and dotted line are the (E) Gauss and (F) linear functions for all plot marks, respectively.

The fact that $E_{s,0.5}$ is proportional to $\langle u_h \rangle$ suggests that the ratio of $E_s/\langle u_h \rangle$ is an important parameter for the trap. Figure 14 shows the plots of the DNA trap probability as a function of the ratio $E_s/\langle u_h \rangle$ for all data in Figs. 10–12. In this figure, all plots are scattered around a line. This suggests that the trapping probability is determined only by the ratio of $E_s/\langle u_h \rangle$. In Fig. 14, the scattering for the same $\langle u_h \rangle$ and same DNA size is much less than for all data. This suggests that the scattering is mainly caused by inaccuracies of ΔP and $\langle u_h \rangle$ measurement. The accuracies for V_a and E_s are better than for ΔP and $\langle u_h \rangle$ in our setup. Assuming $E_{s,0.5}$ is proportional to $\langle u_h \rangle$, we replotted Fig. 14 as a function of normalized electric field $E_n = E_s/E_{s,0.5}$ instead of $E_s/\langle u_h \rangle$ (Figs. 15–17). The scattering in Fig. 14 is much improved in Figs. 15–17; all data are now on a curve. For further discussion in the future, we obtained the fitting curves for those plots. The solid curves and dashed lines in Figs. 15–17 are the Gaussian and line functions $\beta_G = k_0 \exp[-((E_n - k_1)/k_2)^2] + k_3$ and $\beta_L = k_4 E_n - k_5$, respectively, where β is the trapping probability. Table II indicates the constants of expression for the Gaussian and line functions. Gaussian fitting agrees well with the plots.

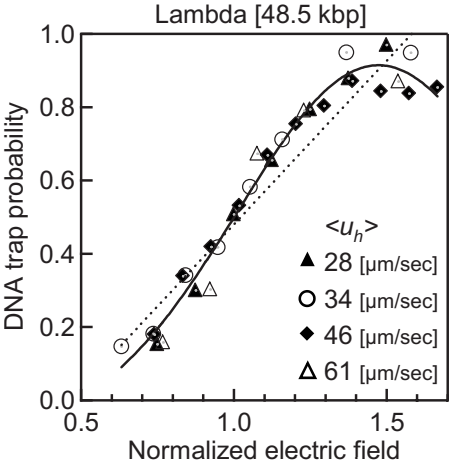

FIG. 16. Trapping probability of lambda DNA versus normalized voltage. The voltage was normalized at the value of 0.5 for the trapping probability at each pressure difference shown in Fig. 11. The solid curve and dotted line are the (C) Gauss and (D) linear functions for all plot marks, respectively.

The values of ΔP and V_a needed to trap different sizes of DNA increase with the DNA size, as shown in Figs. 10–12. In other words, the absolute values of ΔP and V_a are important for trapping different sizes of DNA molecules. In contrast, Figs. 14–17 strongly suggest that the trapping probability is determined only by the ratio of $E_s/\langle u_h \rangle$. This is informative when we are considering the trapping mechanism. From this finding, we suggest that the dielectrophoretic force is not dominant in our trap and the streamline of the DNA driven by two forces, which is determined only by the ratio of $E_s/\langle u_h \rangle$, regulate the trapping probability. Due to our interest in the mechanism, we measured the dc-DEP, hydrodrag, and Lorentz forces on the DNA in the conditions of our

TABLE II. Constants of fitted Gaussian and line functions. This table indicates the constants $(k_0 - k_5)$ of expressions for the Gaussian and line functions $\beta_G = k_0 \exp[-((E_n - k_1)/k_2)^2] + k_3$ and $\beta_L = k_4 E_n - k_5$, respectively, which are used in Figs. 15–17 as fitting functions. β is the trapping probability, and E_n is the normalized voltage.

	Gaussian				Line	
	k_0	k_1	k_2	k_3	k_4	k_5
			(A)			(B)
T4	0.84	1.29	0.34	−0.10	1.36	0.85
			(C)			(D)
Lambda	1.02	1.47	0.63	−0.10	0.89	0.41
			(E)			(F)
M13mp9	0.78	1.27	0.30	0.16	1.61	1.09

experiment and also performed three-dimensional (3D) numerical simulation. The results shall be published elsewhere.

V. CONCLUSIONS

We developed an analysis method to statistically obtain the trapping probability of a DNA trap from the fluorescence gradient in a microfluidic channel. We measured the trapping probability as a function of DNA size, electric field, and average hydraulic velocity. The trapping probability increases with the electric field and average hydraulic velocity. A larger electric field and hydraulic velocity are required for trapping smaller-sized DNA. The trap probability can be used as a quantitative indicator to optimize this method for potential applications, such as the extraction, concentration, and purification of DNA/RNA molecules from the lysis solution of a single cell on a chip. The electric field giving the trap probability of 0.5 is proportional to the average hydraulic velocity for all DNA sizes. This revealed that the trap is not simply caused by the balance between the dielectrophoresis and hydrodrag forces. In all measured conditions and accuracy, the trapping probability is determined only by the ratio of the electric field to the average hydraulic velocity. These results are helpful toward discussing the mechanism of the trap.

ACKNOWLEDGMENTS

This work was partially supported by PRESTO (Precursory Research for Embryonic Science and Technology), Japan Science and Technology, and grants-in-aid for scientific research from the Ministry of Education, Culture, Sports, Science and Technology of Japan.

[1] W. D. Volkmuth and R. H. Austin, Nature (London) **358**, 600 (1992).
[2] S. W. Tuner, A. M. Perez, A. Lopez, and H. G. Craighhead, J. Vac. Sci. Technol. **B38**, 3835 (1998).
[3] J. Han and H. G. Craighead, Science **288**, 1026 (2000).
[4] M. Ueda, T. Hayama, Y. Takamura, Y. Horiike, and Y. Baba, Electrophoresis **23**, 2635 (2002).
[5] T. Sano, N. Iguchi, K. Iida, T. Sakamoto, M. Baba, and H. Kawaura, Appl. Phys. Lett. **83**, 4438 (2003).
[6] Y. Takamura, T. Havama, M. Ueda, Y. Baba, and Y. Horike, in Proceedings of the μTAS, 2002, Nara, Japan, edited by Y. Baba *et al.* (The University of Tokushima, Japan, 2002), Vol. 1, p. 317.
[7] Y. Takamura, Y. Horiike, Y. Baba, and E. Tamiya, in Proceedings of the μTAS, 2003, California, USA, edited by M. Allen Northrup *et al.* (MicroFluidic Systems Inc., San Diego, 2003), Vol. 1, p. 317.
[8] Y. Tomizawa, K. Yuhki, Y. Morita, E. Tamiya, and Y. Takamura, Proceedings of the μTAS, 2004, Malmö, Sweden, edited by T. Laurell *et al.* (Lund Institute of Technology, Sweden, 2004), Vol. 1, p. 659.
[9] K. Yuhki, Y. Tomizawa, Y. Morita, E. Tamiya, and Y. Takamura, in Proceedings of the μTAS, 2004, Malmö, Sweden, edited by T. Laurell *et al.* (Lund Institute of Technology, Sweden, 2004), Vol. 2, p. 294.
[10] Y. Tomizawa, H. Oose, K. Ueno, M. S. Ahsans, N. Nagatani, W. Nagasaka, E. Tamiya, and Y. Takamura, in Proceedings of the μTAS, 2006, Tokyo, Japan, edited by T. Kitamori *et al.* (The University of Tokyo, Japan, 2006), Vol. 1, p. 659.
[11] Y. Takamura, W. Nagasaka, K. Ueno, Y. Tomizawa, and E. Tamiya, in Proceedings of the μTAS, 2007, Paris, France, edited by Jean-Louis Viovy *et al.* (Institute Curie, France, 2007), Vol. 2, p. 1429.
[12] M. Washizu and I. Turosawa,IEEE Trans. Ind. Appl. **26**, 1165 (1990).
[13] C. F. Chou, J. O. Tegenfeldt, O. Bakajin, S. S. Chan, E. C. Cox, N. Darnton, T. Duke, and R. H. Austin, Biophys. J. **83**, 2170 (2002).
[14] C. L. Asbury, A. H. Diercks, and G. Engh, Electrophoresis **23**, 2658 (2002).
[15] S. Tuukkanen, J. J. Toppari, A. Kuzyk, L. Hirviniemi, V. P. Hytolnen, T. Ihalainene, and P. Trm, Nano Lett. **6**, 1339 (2006).